Applicability of the global TanDEM-X elevation data for terrain modelling of a forested karst area: a case study from Slovak Karst

Peter BANDURA, Michal GALLAY

Abstract: *New interferometric radar data of the TanDEM-X space mission have become recently available as a global digital elevation model providing 0.4 arc second spatial resolution (ca. 12 meters). The TanDEM-X dataset brings new options into geoscientific research across multiple scales. However, the accuracy and suitability of this data have not been evaluated in such an extensive manner as, for example, the widely used SRTM data which resolution is 1 arc second (ca. 30 m). We present a validation of the vertical accuracy of TanDEM-X DEM product and an evaluation of its suitability for landform classification in a forested karst area. The DEM segmentation using geomorphons was used for the automated object-based landform classification. We focused on the identification of dolines for which polygons of dolines mapped by an expert-driven approach were used for validation. Airborne lidar data in the form of DSM and DTM were used as the reference dataset for validation of the TanDEM-X DEM vertical accuracy. The results from the study area show that the vertical RMSE of the TanDEM-X data is 3.42 m with respect to the lidar DSM and 9.64 m in comparison with lidar DTM. The identification of dolines by the geomorphon approach achieved 73 % with TanDEM-X, lower than for the lidar DTM (85 %). The TanDEM-X elevation errors were strongly correlated with the canopy height derived from the lidar data suggesting limited suitability of the TanDEM-X data for mapping fine-scale geomorphological features under forests while there was a good match with the lidar DTM terrain in open areas.*

Keywords: *terrain, doline, radar interferometry, geomorphon, accuracy, lidar*

Introduction

Synthetic aperture radar interferometry (InSAR) is one of the most applicable remote sensing technologies for acquiring land surface elevation data for the entire Earth. It is an active method capable of mapping the land surface independent of daytime and weather conditions. The InSAR uses microwave energy pulses which can penetrate through clouds and in some extent the forest canopy (e.g., Farr et al. 2007, Rott 2009). The technology has been successfully deployed in 2000 by the NASA Shuttle Radar Topographic Mission (SRTM) for acquiring an elevation dataset of a near-global coverage with 1 arc second spatial resolution (ca. 30 meters) and vertical accuracy of below 10 meters (Farr et al. 2007, NASA 2013). The digital elevation model (DEM) derived from the SRTM data has become the most well-known and most widely used digital elevation model (DEM) for geomorphometric analysis of the land surface.

A much higher level of detail and accuracy of elevation data has been achieved by the TanDEM-X mission of the German Aerospace Center (DLR) and its partners. The mission operates a twin constellation of Terra-SAR-X and TanDEM-X satellites orbiting the Earth in a helix formation. Both sensors of the TanDEM-X mission can transmit and receive the electromagnetic wave with a phased-array X-band antenna with a carrier frequency of 9.65 GHz resulting in a wavelength of about 3.1 cm (Gruber et al. 2012, Krieger et al. 2013).

DOI: https://doi.org/10.33542/GC2022-1-03

The global TanDEM-X digital elevation data were collected for the entire land surface of the Earth during 2010-2014 in at least two or up to four overpasses at 0.4 arc second spatial resolution and a claimed relative vertical accuracy below 2 meters on slopes inclined less than 11° and an absolute vertical accuracy of 10 m (Wessel et al. 2018, Grohmann 2018, Zhang et al. 2019). The TanDEM-X DEM is distributed by DLR (2016) via proposal submission for scientific users or commercially as the WorldDEM product by the Airbus Defence and Space. As with other SAR elevation products, the measured values are samples of the land cover surface elevations thus being a digital surface model (DSM) including buildings and trees. The elevation values represent the ellipsoidal heights of the land cover surface relative to the WGS84 ellipsoid in the WGS84-G1150 datum. The TanDEM-X Digital Elevation Model is not edited and therefore can contain radar and processing artefacts as well as voids. Nevertheless, the data have opened new horizons in global applications of geomorphometry. TanDEM-X data first stimulated research on geometric and semantic accuracy of the product in various kinds of environments including high mountains and urban landscape (Rexer and Hirt 2016, Schreyer and Lakes 2016, Chu and Lindenschmidt 2017, Purinton and Bookhagen 2017, Wessel et al. 2018, Grohmann 2018). Some of the validation studies are based on comparison with other global DEM products such as SRTM, ASTER GDEM, or ALOS World 3D of coarser resolution than of TanDEM-X data. Also, GNSS measurement on points or along lines have been used are used (Purinton and Bookhagen 2017). In this case, GNSS reference measurements are based on point sample support whereas the SAR elevation measurement refers to an area where the average of elevation within the instantaneous field of view is recorded. The lidar coverage provides means for upscaling the reference elevation for both DTM and DSM to closely approximate the support of the TanDEM-X data. This approach was rarely exploited to date (e.g. Schreyer and Lakes 2016). Given that TanDEM-X DEM represents a DSM, for geomorphologic studies, it is crucial to analyse its semantic accuracy of identification of landforms associated with the terrain surface. This was the motivation of Hengl and Reuter (2011) for comparing the accuracy of the GDEM (Global DEM product) and its usability in the watershed analysis against the reference lidar DEM.

Therefore, we focused this study on a partially forested karst area for which a high-resolution lidar coverage exists (Hofierka et al. 2018) to validate the TanDEM-X DEM data in terms of vertical accuracy and semantic accuracy. The latter aspect was based on the identification of karst depressions (dolines) by the means of the Geomorphons concept introduced by Jasiewicz and Stepinski (2013). The area of interest is abundant with dolines, specific karst depressions which control the overland flow of water in a karst region (Hofierka et al. 2018), indicate the rate of chemical erosion (Chamberlin et al. 2019), structural rock properties (Telbisz et al. 2016, Öztürk et al. 2018), or serve as refugees for some biological species (Raschmanová et al. 2018, Bátori et al. 2019). Therefore, dolines are of interest in landform identification.

Study area

The area of interest (4.5 × 7 km) is a part of the Slovak Karst (Slovenský kras) near the state border of Slovakia with Hungary, Central Europe (Fig. 1). The area comprises the Silická planina Plateau with gradually decreasing altitude from 600 m a.s.l. in the north to about 305 m a.s.l. in the south. Dolines and sinkholes of blind valleys including caves are typical landforms in the area. The landscape evolved on carbonate rocks comprising mainly Triassic limestones and dolomites of the Silica Nappe. The land is covered by deciduous forests (70%) where oak and hornbeam are the most common species (Balogh and Barabas 2016). The rest of the study area comprises grassland (20%), shrubs (6%), and arable land (1%), built-up (1%), and other areas).

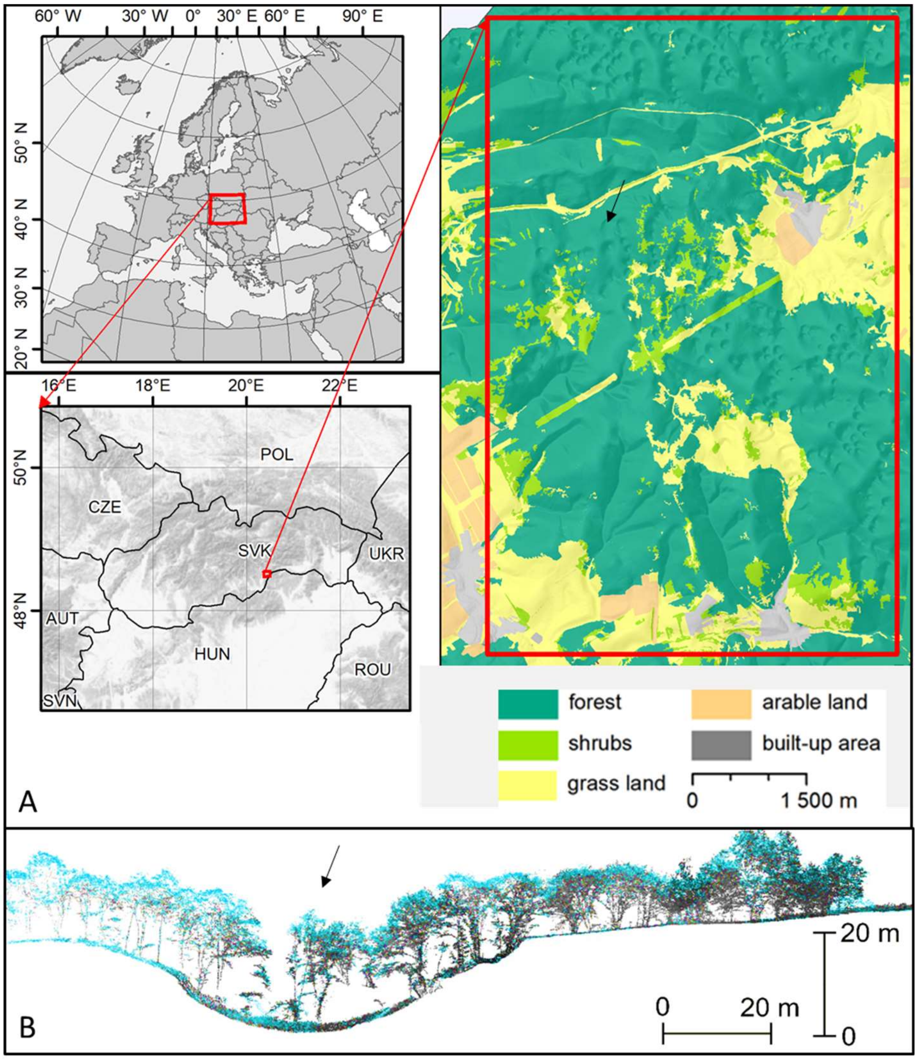

Fig. 1. *Location of the area of interest and its land cover valid to 2015 (A). The black arrow shows the location of a doline in (B) which is displayed as a vertical cross-section of a lidar point cloud. Cyan points were recorded by airborne laser scanning in 2014 while black points originated from terrestrial laser scanning.*

Input data

The DSM and DTM derived from an airborne lidar point cloud originated within an airborne laser scanning mission flown in August 2014, were used as the reference DEMs. The average density of all laser returns was 29 points/m^2 while it was 21 points/m^2 for the last returns only. The majority of the area is forested, therefore, the average density of ground returns is 4 points/m^2, but the minimum is not lower than 0.5 points/m^2. The accuracy of measurement in open areas is reported at 0.1 m (1σ) by the data supplier. Further details see in Hofierka et al. (2017, 2018). The first returns and ground returns were used to produce the DSM and DTM, respectively. These models were derived by direct point-to-grid conversion into a squared grid of 12 m cell size with the las2grid module in LAStools (Isenburg 2014).

The sampling support for the SAR method is an area approximately in the size of a TanDEM-X data cell, therefore the values of the cells in the lidar DTM (Fig. 2A) and DSM (Fig. 2B) were calculated as the average Z coordinate (Baltic vertical datum after adjustment) of the lidar points within each cell. The original points and also the derived elevation grids were measured in the national cartographic projection system S-JTSK Krovak EastNorth (EPSG: 5514). The land cover canopy height model (CHM), i.e. normalized height model, was generated by subtracting lidar DTM from the lidar DSM in a map algebra operation (Fig. 2D).

For the entire territory of the Slovak Republic to date, a new airborne lidar coverage is being gradually generated by the Institute of Geodesy, Cartography, and Cadastre of the Slovak Republic (UGKK) with average density of points of 10-30 points/m^2. Although the area of interest in this study has been mapped by the governmental lidar campaign in 2021, we made use of a custom airborne lidar data (Hofierka et al., 2018) with the quality similar to what is being generated by the UGKK and with similar data currency to the TanDEM-X data.

The evaluated TanDEM-X product was a data tile TDM1-DEM-04-N48E020-V01-C, a global standard product derived from multiple TanDEM-X DEM acquisitions within 2011-2013 (© DLR 2016). The data was originally supplied with a spatial resolution of 0.4″ by 0.6″ resolution which corresponds to approximately 12 m cell size. The data were provided by the DLR in WGS 84 geographic coordinate system (EPSG: 4326) with elevations referring to ellipsoidal heights above the WGS 84 spheroid (Fig. 2C).

For comparison, all datasets had to be transformed into the same vertical and horizontal datum. To match the horizontal datum, we projected the TanDEM-X data to S-JTSK Krovak EastNorth (EPSG: 5514) at a 12 m resolution using the bilinear resampling of elevations. The lidar DSM and DTM were kept in S-JTSK EastNorth (EPSG: 5514) but their vertical datum was converted to ETRS89 geographic coordinate system with ellipsoidal heights (EPSG:4258) using the online transformation service of the Slovak Geodetic and Cartographic Institute (GKU 2018). The lidar DSM and DTM were resampled to 12 by 12 m grid resolution using bilinear interpolation.

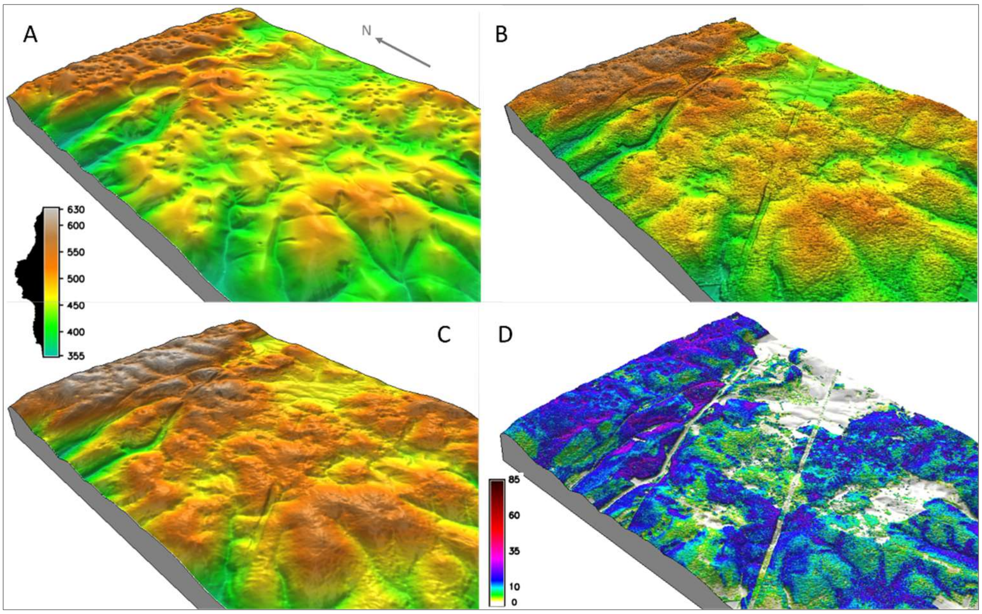

Fig. 2. *3D perspective views of (A) the lidar DTM, (B) lidar DSM, (C) TanDEM-X DEM coloured by elevation and (D) lidar DSM coloured by lidar-derived canopy height. All models are derived at 12 meters spatial resolution.*

Vertical accuracy assessment and classification of landforms

Validation of the vertical accuracy was based on vertical errors calculated as grid-to-grid comparison in the map algebra subtraction of the lidar DSM and lidar DTM from the TanDEM-X DEM, respectively. Reference data comprised doline polygons as presented in Hofierka et al. (2018). They used overlayed slope gradient, mean curvature, and hill-shade layers to manually delineate the dolines by expert judgment. The polygons were converted into circles centered at the polygon centroids. The reason was that the circular shape of dolines suited the raster-based analyses involved in the workflow. Overall, there are 311 manually delineated dolines within our study area with a mean area size of 9238.13 m^2 and a mean radius of 62.94 m.

The r.geomorphon module in GRASS GIS (GRASS Development Team 2018) was used for automated landform classification. Geomorphons is a relatively new method employing the concept of topographic pattern recognition, using only DEM as input data (Jasiewicz and Stepinski 2013). In short, the algorithm looks from the focus cell in eight principal directions and designates whether the neighbouring cells are higher, lower, or the same height as the central cell. Then, based on the pattern of the neighbouring cells, labels the focal one with one of the ten general landforms (pit or depression being the case of dolines). The calculation depends on the four main parameters: outer search radius (search), inner search radius (skip), flatness threshold (flat), and flatness distance (dist). Three different settings of search radiuses, targeted to the recognition of the dolines, using the value of the mean radius of the reference dolines (6 cells) were tested here (the other parameters were left as default):

Test 1: search = 6 cells (as mean radius), skip = 0;
Test 2: search = 12 cells (as double the mean radius), skip= 0;
Test 3: search = 12 cells (as double the mean radius), skip = 6 (as mean radius).

Depressions classified by the geomorphons method within the area of karstified carbonate bedrock were converted into polygons and compared with the reference polygons. Next, geomorphons classes were assigned to the centroids of the reference polygons, and their membership to the depression class was evaluated. Also, the Compute Confusion Matrix tool in the Spatial Analyst Extension in ArcGIS 10.4 (ESRI 2016) was used for accuracy assessment of overall landforms classification obtained by the geomorphons method. There were 100 points distributed randomly within each of the ten landform classes, using the equalized stratified random sampling. The accuracy of the classifications was computed for Lidar DTM vs. TanDEM-X DEM, considering the classification of the lidar DTM as the reference dataset.

Results and Discussion

The statistical analysis indicates that TanDEM-X data more closely approximates the land cover surface and largely overestimates the terrain surface (Tab. 1). This fact is apparent looking at the measures of central tendency, such as the mean and median error, having a positive value of around 7.5 m for the lidar DTM. The RMSE of 9.64 m with respect to the DTM also indicates a large overall deviation of the TanDEM-X surface from the reference lidar DTM. Statistics for the vertical errors with respect to the lidar DSM show a narrower spread of height differences. Fig. 3 shows the spatial distribution of the vertical errors which can be compared with the lidar canopy height model (CHM). The differences between TanDEM-X DEM and lidar DSM and DTM are within a metre in the areas of low CHM values (open land surface). On the other hand, the differences are larger in the forested areas where the CHM values are high. Fig. 3 can be compared with Fig. 1 where the land cover is displayed.

Tab. 1. *Vertical accuracy assessment of the TanDEM-X DEM against the lidar DSM and lidar DTM*

Statistics	TanDEM-X - lidar DSM	TanDEM-X - lidar DTM
Count	218 750	218 750
Min (m)	-19.54	-6.14
Max (m)	27.10	36.91
Mean (m)	-1.99	7.54
SD (m)	2.78	6.01
RMSE (m)	3.42	9.64
Median (m)	-1.84	7.53

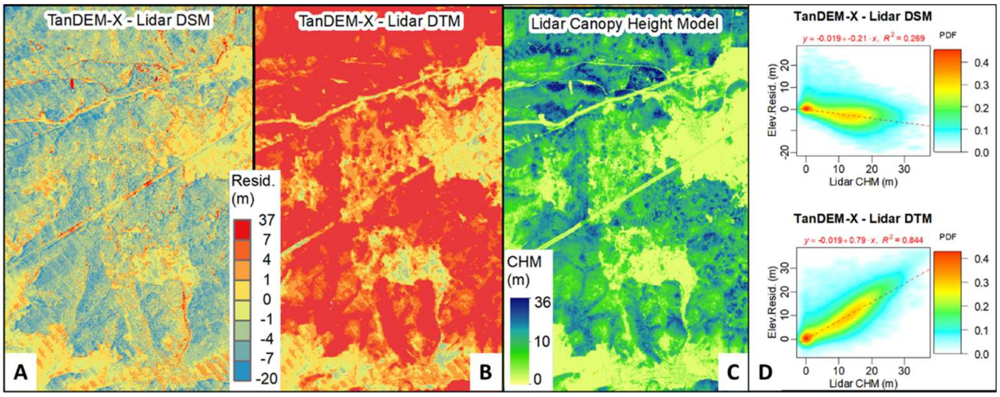

Fig. 3. *Vertical errors of the TanDEM-X elevation data with respect to (A) the lidar DSM and (B) lidar DTM, respectively; (C) Landscape canopy height (CHM) and (D) its linear relationship with the errors a bivariate scatterplot of probability density*

While the TanDEM-X underestimates the DSM in the forested land for which the errors are negative, it overestimates the Lidar DTM in the forested areas where the errors become positive. The relationship between the errors with respect to the DSM and DTM and the CHM is depicted by the scatterplots (Fig. 3D) showing pairs of cell values where the points are mapped by a probability density function (PDF). A high concentration of point pairs is indicated by yellow to red tones. While the relationship is negative though weak for the DSM-based errors, the DTM-based errors show a strong correlation with CHM which is significant at $p = 0.01$. This indicates that TanDEM-X DEM data in the study area do not represent the ground surface (terrain) but the canopy surface which poses possible limitations to accurately identifying the terrain features in forested land. Similar findings were reported by Chu and Lindenschmidt (2017). General overestimation of the reference terrain surface by the TanDEM-X can be also observed in Figure 4 where the errors concentrate around zero for open land while they are shifted towards higher positive values in forested areas. The relatively large negative errors between TanDEM-X and Lidar DSM (below -7 m) occur in the forested areas indicating that TanDEM-X underestimates the forest canopy with respect to the Lidar DSM (Fig. 3A, 3C, 4B, 5B). This finding can be related to the penetration of the X-band radar wavelengths into the tree canopy until the signal is scattered back. Values of -6 m were reported by Kellndorfer et al. (2004) and Solberg et al. (2007) for the SRTM C-band and X-band, respectively. It is also reported by Gdulová et al. (2020) for TanDEM-X data from the Krkonoše and Šumava mountains in Czechia. Lower negative values in our case can also be related to systematic underestimation on slopes particularly orientated off the signal direction inducing radar signal shadow and also to the leaf-on/leaf-off condition during the time of sensing.

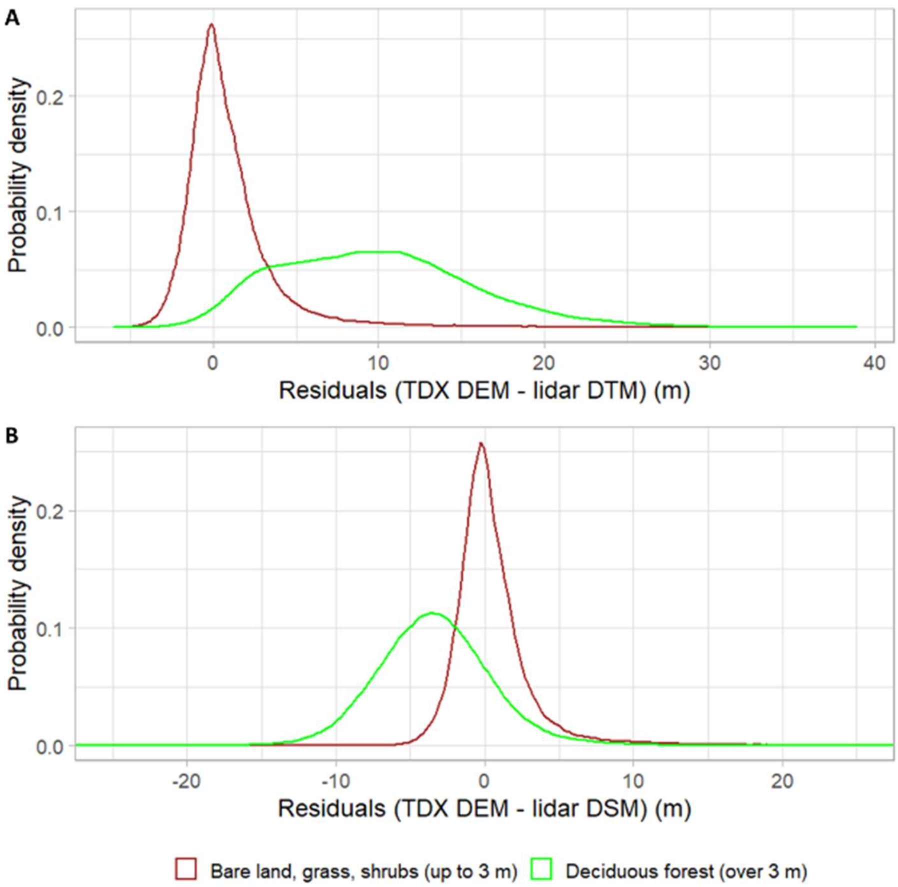

Fig. 4. *Distribution of vertical errors for TanDEM-X DEM with respect to (A) lidar DTM and (B) lidar DSM, respectively*

Figures 5 and 6 show the boxplots of vertical errors stratified according to 16 slope aspect categories based on land cover (Fig. 5) and 3 slope angle categories (Fig. 6). The independency of slope aspect and slope angle and slope angle and land cover was checked by calculating the circular vs. linear variable correlation coefficient and Spearman's rank coefficient, respectively, using the R package "Directional" and "base". The correlation of both pairs of variables resulted in 0.013 and 0.382, respectively, having a p-value below 0.0001. Based on the results, we claim there is a very weak and weak correlation between the tested variables, respectively. Figure 5 illustrates the lower spread of vertical errors and low mean residuals for open land as opposed to forested land regardless of the reference DEM, whether it is DTM (Fig. 5A) or DSM (Fig. 5B). The vertical errors tend to increase for both reference surfaces (Fig. 6A, 6B) with increasing slope angle. The median vertical errors and RMSE for the two slope categories follow the results reported in Wessel et al. (2018), Grohmann (2018), Zhang et al. (2019), Gdulová et al. (2020).

The errors are highest for N, NE oriented slopes (0° – 67.5°) for the reference DTM (Fig. 6A). On the other hand, the highest errors for the reference DSM (Fig. 6B) tend to concentrate in the opposite W, SW direction (202.5° – 270°). This trend is preserved also in Fig. 5 thus it cannot be explained by land cover or slope individually. The correlation of larger errors in TanDEM-X DEM with westerly facing and relatively steep slopes was also found by Gdulová et al. (2020). The authors relate the findings to the effect of look angle direction and coverage by the SAR signal with a single mode of scanning (ascending or descending), which can also explain the distribution of errors in our study area.

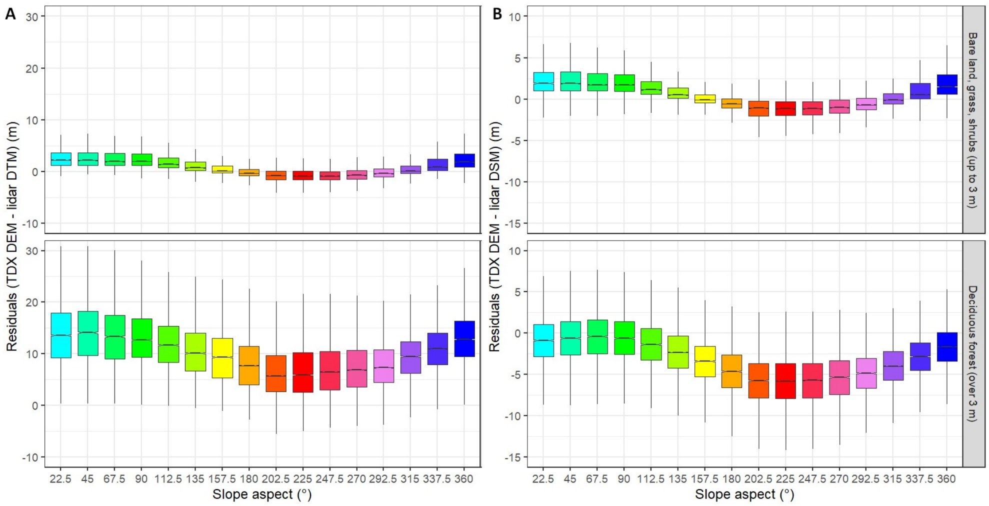

Fig. 5. *The vertical errors between (A) TanDEM-X DEM and LiDAR DTM, (B) TanDEM-X DEM and LiDAR DSM in relation to land cover in the study area against the slope aspect*

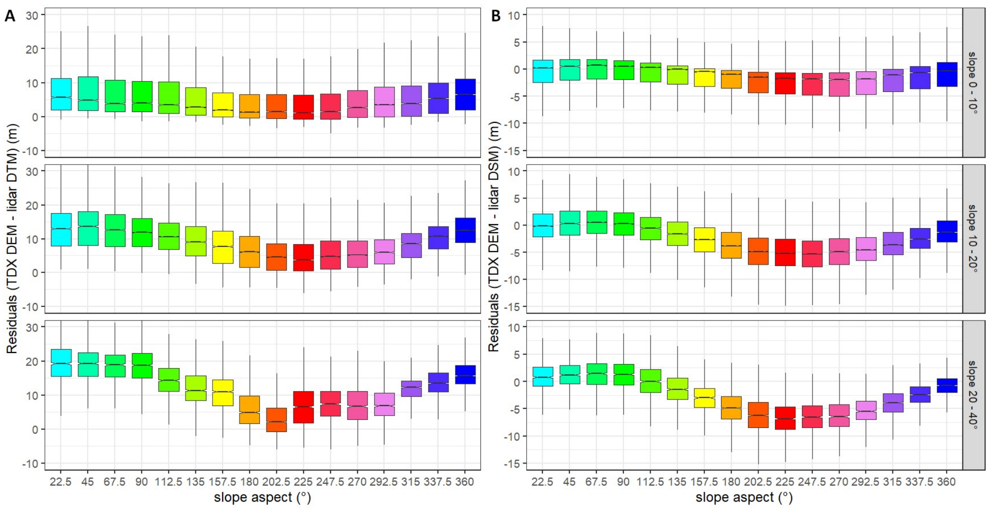

Fig. 6. *The vertical errors between (A) TanDEM-X DEM and Lidar DTM, (B) TanDEM-X DEM and Lidar DSM in relation to land cover in the study area against the slope angle*

The TanDEM-X elevation surface model was subject to landform segmentation using the method of geomorphon classification in 3 tests. Landforms with planimetrical sizes up to 60 meters were delineated in Test 1. However, the size of the classified depressions does not visually correspond with the reference polygons. The size of the landforms was therefore doubled in Test 2, but the results were still not satisfying. Adjusting also the inner search radius in Test 3 proved to be important for the increase of the size of classified landforms (Fig. 7). Therefore, only classification resulting from Test 3, where landforms with planimetric sizes up to 120 meters and not smaller than 60 meters were delineated, was taken for further analyses. The comparison of reference polygons and polygonal representation of depressions derived by the geomorphons in Test 3 settings are displayed in Fig. 8 and in Table 2. The spatial match was based on the condition of the intersection between the 311 reference polygons and the doline polygons resulting from the DTM classification. The highest number of depressions within the area of karstified carbonate bedrock was derived from the lidar DTM (216) of which 85 % of depressions intersect with the reference doline polygons. However, their mean area and diameter are markedly smaller than th reference, which points to their underestimation given by the settings of calculation of geomorphons. As expected, the number of matching depressions mapped from the TanDEM-X is smaller, but still acceptable 157 and its 73 % of the reference polygons.

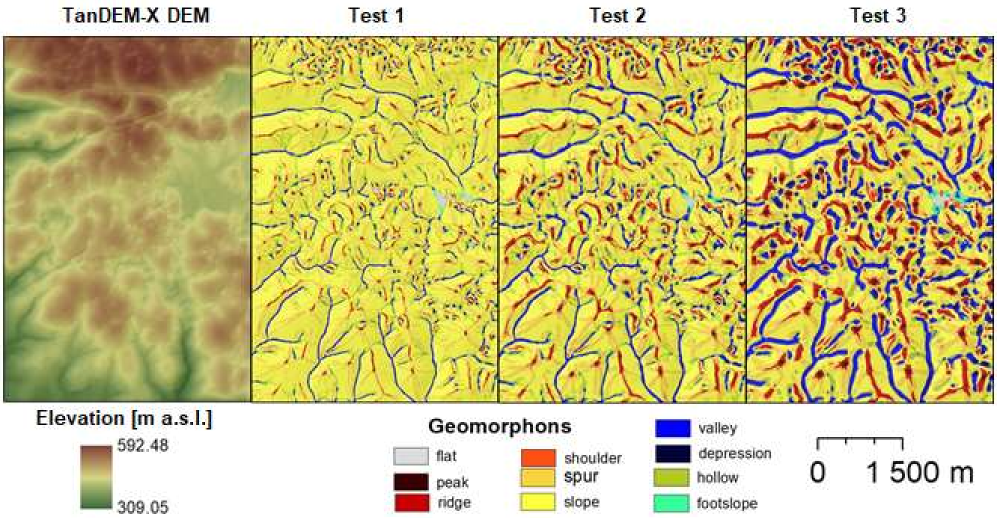

Fig. 7. *Landform classification of the TanDEM-X DEM based on various input parameters setting (Test 1 – 3, details see in the text) resulting in 10 classes of geomorphons.*

Tab. 2. *Summary statistics of reference doline polygons and depressions classified by the geomorphons method within the area of the karstified carbonate bedrock*

Input DTM		Geomorphons			
		Lidar		TanDEM-X	
Reference data		All	Int	All	Int
Count	311	216	184	157	114
Mean area (m^2)	9205.73	2947.22	3021.20	2797.45	3110.53
Mean d (m)	108.26	61.52	62.02	59.68	62.93
%	-	-	85.19	-	72.61

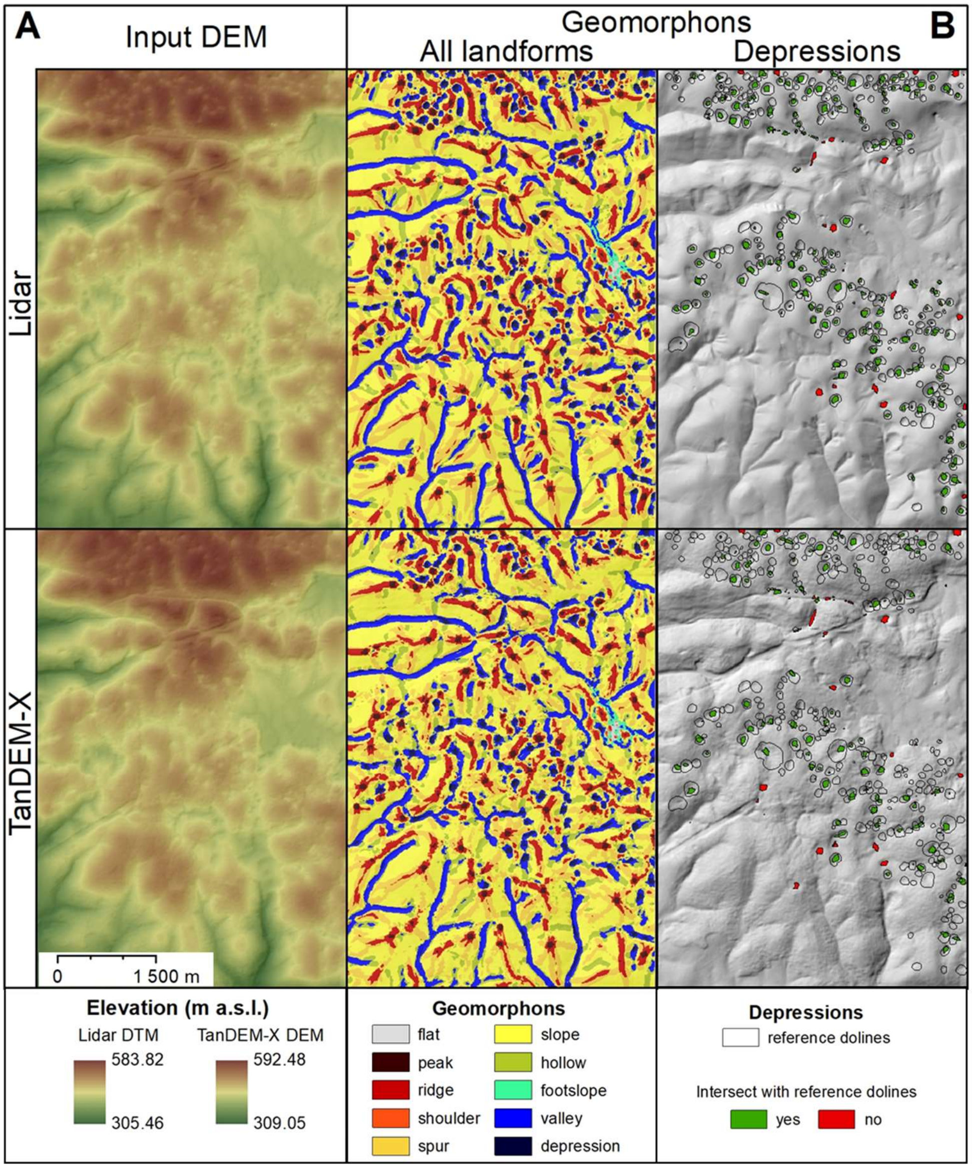

Fig. 8. *Landform classification based on (A) the input lidar DTM and TanDEM-X DEM resulting in (B) 10 classes of geomorphons (input parameters setting Test 3) from which the class "depression" was extracted and compared as an intersection with the reference doline polygons*

The proportion of correctly classified dolines decreased if the measure of accuracy is targeted precisely to the centroids of the reference polygons (Table 3). For the lidar DTM, the spatial match achieved 62 % and 33 % for the TanDEM-X DEM. The remaining dolines are classified as the landforms of the valley, hollow, slope, and spur. It can be also related to the settings of geomorphons calculation. Small dolines can be classified and mapped as a valley or slope if the inner or outer search radius values are set to large. It applies also to the larger dolines if the search radiuses are too small.

***Tab. 3.** Centroids of reference polygons with assigned landform classes by the geomorphons method for the input Lidar DTM and TanDEM-X DEM*

Class of geomorphons	Input DEM			
	Lidar		TanDEM-X	
	N	%	N	%
Ridge	0	0.00	10	3.22
Spur	1	0.32	17	5.47
Slope	10	3.22	55	17.68
Hollow	22	7.07	43	13.83
Footslope	0	0.00	0	0.00
Valley	84	27.01	82	26.37
Depression	194	62.38	104	33.44
Total	311		311	

% – Percent of total number of centroids (311)

Tab. 4 assesses the accuracy of detecting the depression class by the geomorphon method in the TanDEM-X DEM. The overall assessment of the accuracy of the geomorphons classification (Kappa index of agreement) against the Lidar DTM is 0.46. The accuracy of detecting the class "depression" is slightly higher (0.5 for TanDEM-X DEM), though it is generally low. The geometric accuracy, precision, and geomorphic level of detail preserved in the lidar DTM is even after the resampling to 12-meter resolution still better than compared to the TanDEM-X surface.

***Tab. 4.** Confusion matrix of classification accuracy assessment for the class depression derived by the geomorphon method from the TanDEM-X DEM against the Lidar DTM*

Confusion matrix		Depression landforms from TanDEM-X DEM
Count	Reference depressions from Lidar DTM	100
	True positives	50
	False positives	5
	All detected depressions from TanDEM-X DEM	55
Accuracy	Producer´s	0.50
	User´s	0.91

Conclusions

We analyzed the TanDEM-X elevation dataset for karst, a largely forested landscape in Slovakia. The results showed this digital elevation model largely overestimates the terrain surface where the forest grows. The TanDEM-X represents the canopy surface albeit it underestimated it by a few meters under on average in the study area with leaf-on tree conditions. These findings follow previous similar studies. From the perspective of landform classification, the reported facts pose limitations which were shown by the geomorphons classification targeted at the recognition of dolines. Future research should focus on testing the settings for extracting the geomorphons at the spatial scale relevant to the objects of interest and the source DTM. In terms of TanDEM-X vertical error assessment, it should focus on areas with a low percentage of canopy, e.g. mountainous areas, where, on the other hand, a problem of radar shadow can arise. Nevertheless, the TanDEM-X digital elevation dataset is being corrected and processed similarly to the SRTM improvement to represent the land surface more accurately. The data will truly bring revolution into planetary terrain analysis in high spatial resolution or in spatial prediction such as soil properties where no in-situ sample network exists (Cherlinka et al., 2019). Regional or state-wide assessment of TanDEM-X height and positional error will be possible also in Slovakia as the national lidar data covers already the majority of the state and should become complete by 2023.

References

BALOGH, M., BARABAS, D. 2016: Analysis of species composition of tree cover in the area of Slovak Karst (Slovenský kras). *Geographia Cassoviensis*, 10(2), 93-106.

BÁTORI, Z., VOJTKÓ, A., MAÁK, I.E., LŐRINCZI, G., FARKAS, T., KÁNTOR, N., TANÁCS, E., KISS, P.J., JUHÁSZ, O., MÓDRA, G., TÖLGYESI, C., ERDŐS, L., AGUILON, D.J., KEPPEL, G. 2019: Karst dolines provide diverse microhabitats for different functional groups in multiple phyla. *Scientific Reports*, 9, 7176.

CHAMBERLIN, C.A., BIANCHI, T.S., BROWN, A.L., COHEN, M.J., DONG, X., FLINT, M.K., MARTIN, J.B., MCLAUGHLIN, D.L., MURRAY, A.B., PAIN, A., QUINTERO, C.J., WARD, N.D., ZHANG, X., HEFFERNAN, J.B. 2019: Mass balance implies Holocene development of a low-relief karst patterned landscape. *Chemical Geology*, 527, 118782. DOI: https://doi.org/10.1016/j.chemgeo.2018.05.029.

CHERLINKA Vasyl, DMYTRUK Yuriy, BARABAS Dušan 2019: Methods of verification of soils prediction maps: a case study from Chernivtsi region, Ukraine. *Geographia Cassoviensis*, 13(2), 141-160.

CHU, T., LINDENSCHMIDT, K.-E. 2017: Comparison and Validation of Digital Elevation Models Derived from InSAR for a Flat Inland Delta in the High Latitudes of Northern Canada. *Canadian Journal of Remote Sensing*, 43(2), 109-123. DOI: https://doi.org/10.1080/07038992.2017.1286936.

DLR 2016: *TanDEM-X DEM – An-nouncement of Opportunity*. Wessling (DLR – Deutsches Zentrum für Luft- und Raumfahrt). Available at: https://tandemx-science.dlr.de/pdfs/TD-GS-PS-0021_DEM-Product-Specification_v3.1.pdf.

ESRI 2016: *ArcGIS Desktop: Release 10.4*. Environmental Systems Research Institute, Redlands, CA, USA.

FARR, T. G., ROSEN, P. A., CARO, E., CRIPPEN, R., DUREN, R., HENSLEY, S., KOBRICK, M., PALLER, M., RODRIGUEZ, E., ROTH, L., SEAL, D., SHAFFER S., SHIMADA, J., UMLAND, J., WERNER, M., OSKIN, M., BURBANK, D., ALSDORF, D. 2007: The shuttle radar topography mission. *Reviews of Geophysics*, 45, 1-33. https://doi.org/10.1029/ 2005RG000183.

GDULOVÁ, K., MAREŠOVÁ, J., MOUDRÝ, V. 2020. Accuracy assessment of the global TanDEM-X digital elevation model in a mountain environment, *Remote Sensing of Environment*, 241. DOI: https://doi.org/10.1016/j.rse.2020.111724.

GKU 2018: *Rezortná transformačná služba*. Retrieved from: https://zbgis.skgeodesy.sk/rts /sk/Transform.

GRASS Development Team 2018: *Geographic Resources Analysis Support System (GRASS) Software*, Version 7.4. Open Source Geospatial Foundation. https://grass.osgeo.org

GROHMANN, C. H. 2018: Evaluation of TanDEM-X DEMs on selected Brazilian sites: Comparison with SRTM, ASTER GDEM and ALOS AW3D30, *Remote Sensing of Environment*, 212, 121-133.

GRUBER, A., WESSEL, B., HUBER, M., ROTH, A. 2012: Operational TanDEM-X DEM calibration and first validation results. *ISPRS Journal of Photogrammetry and Remote Sensing*, 73, 39-49. DOI: https://doi.org/10.1016/j.isprsjprs.2012.06.002.

HENGL, T., REUTER, H.I. 2011: How accurate and usable is GDEM? A statistical assessment of GDEM using Lidar data. In Hengl, T., Evans, I. S., Wilson, J. P., Gould, M. eds. *Geomorphometry 2011 Conference Proceedings*. ESRI (Redlands).

HOFIERKA, J., GALLAY, M., BANDURA, P., ŠAŠAK., J. 2018: Identification of karst sinkholes in a forested karst landscape using airborne laser scanning data and water flow analysis. *Geomorphology*, 308, 265-277. DOI: https://doi.org/10.1016/j.geomorph.2018.02.004.

HOFIERKA, J., GALLAY, M., KAŇUK, J., ŠAŠAK, J. 2017: Modelling Karst Landscape with Massive Airborne and Terrestrial Laser Scanning Data. In Ivan, I., Singleton, A., Horák, J., Inspektor, T. eds. *The Rise of Big Spatial Data, Lecture Notes in Geoinformation and Cartography*, Springer International Publishing, 141-154.

ISENBURG, M. 2014: *LAStools - efficient LiDAR processing software* (version 141017, unlicensed). Retrieved from: http://rapidlasso.com/LAStools.

JASIEWICZ, J., STEPINSKI, T.F. 2013: Geomorphons – a pattern recognition approach to classification and mapping of landforms. *Geomorphology*, 182, 147-156. DOI: https://doi.org/10.1016/j.geomorph.2012.11.005.

KELLNDORFER, J., WALKER, W., PIERCE, L., DOBSON, C., FITES, J.A., HUNSAKER, C., VONA, J., CLUTTER, M. 2004: Vegetation height estimation from Shuttle Radar Topography Mission and National Elevation Datasets. *Remote Sensing of Environment*, 93(3), 339-358. DOI: https://doi.org/10.1016/j.rse.2004.07.017.

KRIEGER, G., ZINK, M., BACHMANN, M., BRÄUTIGAM, B., SCHULZE, D., MARTONE, M., RIZZOLI, P., STEINBRECHER, U., WALTER ANTONY, J., DE ZAN, F., HAJNSEK, I., PAPATHANASSIOU, K., KUGLER, F., RODRIGUEZ CASSOLA, M., YOUNIS, M., BAUMGARTNER, S., LÓPEZ-DEKKER, P., PRATS, P., MOREIRA, A. TanDEM-X 2013: A radar interferometer with two formation-flying satellites. *Acta Astronautica*, 89, 83-98. DOI: https://doi.org/10.1016/j.actaastro.2013.03.008.

NASA 2013: NASA Shuttle Radar Topography Mission Global 1 arc second [Data set]. *NASA EOSDIS Land Processes DAAC*. 2013. DOI: https://doi.org/10.5067/MEaSUREs/SRTM/SRTMGL1.003.

ÖZTÜRK, M.Z., ŞENER, M.F., ŞENER, M., ŞIMŞEK, M. 2018: Structural controls on distribution of dolines on Mount Anamas (Taurus Mountains, Turkey). *Geomorphology*, 317, 107-116. DOI: https://doi.org/10.1016/j.geomorph.2018.05.023.

PURINTON, B., BOOKHAGEN, B. 2017: Validation of digital elevation models (DEMs) and comparison of geomorphic metrics on the southern Central Andean Plateau. *Earth Surface Dynamics*, 5(2), 211-237. DOI: https://doi.org/10.5194/esurf-5-211-2017.

RASCHMANOVÁ, N., ŠUSTR, V., KOVÁČ, Ľ., PARIMUCHOVÁ, A., DEVETTER, M. 2018. Testing the climatic variability hypothesis in edaphic and subterranean Collembola (Hexapoda). *Journal of Thermal Biology*, 78, 391-400. DOI: https://doi.org/10.1016/j.jtherbio.2018.11.004.

REXER, M., HIRT, C. 2016: Evaluation of intermediate TanDEM-X digital elevation data products over Tasmania using other digital elevation models and accurate heights from the Australian National Gravity Database. *Australian Journal of Earth Sciences*, 63(5), 599-609. DOI: https://doi.org/10.1080/08120099.2016.1238440.

RODRIGUEZ, E., MORRIS C.H., BELZ J.E. 2006: A global assessment of the SRTM performance. *Photogrammetric Engineering and Remote Sensing*, 72, 249-260. DOI: https://doi.org/10.14358/PERS.72.3.249.

ROTT, H. 2009: Advances in interferometric synthetic aperture radar (InSAR) in earth system science. *Progress in Physical Geography: Earth and Environment*. 33(6), 769-791. DOI: https://doi.org/10.1177/0309133309350263.

SCHREYER, J., LAKES, T. 2016: Deriving and evaluating city-wide vegetation heights from a TanDEM-X DEM. *Remote Sensing*, 8(11), 940. DOI: https://doi.org/10.3390/rs8110940.

SOLBERG, S., WEYDAHL, D.J., NÆSSET, E. 2007: SAR forest canopy penetration depth as an indicator for forest health monitoring based on leaf area index (LAI). In *5th International Symposium on Retrieval of Bio- and Geophysical Parameters from SAR Data for Land Applications*, Bari, Italy, 25-28.

TELBISZ, T., LÁTOS, T., DEÁK, M., SZÉKELY, B., KOMA, Z., STANDOVÁR, T. 2016: The advantage of lidar digital terrain models in doline morphometry compared to topographic map based datasets – Aggtelek karst (Hungary) as an example. *Acta Carsologica*, 45(1), 5-18. DOI: https://doi.org/10.3986/ac.v45i1.4138.

WESSEL, B., HUBER, M., WOHLFART, C., MARSCHALK, U., KOSMANN, D., ROTH, A., 2018: Accuracy assessment of the global TanDEM-X Digital Elevation Model with GPS data. *ISPRS Journal of Photogrammetry and Remote Sensing,* 139, 171-182. DOI: https://doi.org/10.1016/j.isprsjprs.2018.02.017.

ZHANG, K., GANN, D., ROSS, M., ROBERTSON, Q., SARMIENTO, J., SANTANA, S., RHOME, J., FRITZ, C. 2019. Accuracy assessment of ASTER, SRTM, ALOS, and TDX DEMs for Hispaniola and implications for mapping vulnerability to coastal flooding, *Remote Sensing of Environment*, 225, 290-306. DOI: https://doi.org/10.1016/j.rse.2019.02.028.

ZINK, M., MOREIRA, A. 2015: TanDEM-X: A Challenging Radar Mission for Generating a New Earth's Topography. In Jasiewicz, J., Zwoliński, Z., Mitasova, H., Hengl, T. eds. *Geomorphometry for Geosciences.* Poznan (Adam Mickiewicz University in Poznań).

This work was supported by the Slovak Research and Development Agency under contract No. APVV-15-0054 and by the Grant Agency VEGA under contract No. 1/0798/20. The TanDEM-X DEM data were provided by the DLR under the proposal ID: DEM_OTHER1769. We would like to thank the two anonymous reviewers for their comments which helped us to improve the quality of the paper.

Authors´ affiliation

Dr. Peter Bandura
Department of Physical Geography and Geoecology
Faculty of Natural Sciences, Comenius University in Bratislava
Ilkovičova 6, Mlynská dolina, 842 15 Bratislava
Slovakia
peter.bandura@uniba.sk

Dr. Michal Gallay
Institute of Geography
Faculty of Science, Pavol Jozef Šafárik University in Košice
Jesenná 5, 040 01 Košice
Slovakia
michal.gallay@upjs.sk